DEUTSCHES ELEKTRONEN-SYNCHROTRON DESY

DESY SR 90-05
September 1990

Recent Developments in Soft X-Ray Microscopy

C. Kunz

II. Institut für Experimentalphysik, Universität Hamburg

ISSN 0723-7979

NOTKESTRASSE 85 · 2 HAMBURG 52

To be sure that your preprints are promptly included in the HIGH ENERGY PHYSICS INDEX , send them to the following address (if possible by air mail) :

DESY
Bibliothek
Notkestrasse 85
2 Hamburg 52
Germany

DESY SR 90-05
September 1990

I S S N 0723 - 7979

RECENT DEVELOPMENTS IN SOFT X-RAY MICROSCOPY

C. Kunz

II. Institut für Experimentalphysik, Universität Hamburg,
Luruper Chaussee 149, D-2000 Hamburg 50, FRG

ABSTRACT

There is a great effort worldwide to develop new X-ray microscopes both of the imaging and of the scanning type. Undulator radiation from the next generation of high brightness synchrotron radiation storage rings will be the ideal source for such microscopes. As imaging elements, Fresnel zone plates, grazing incidence mirrors and multi-layer coated normal incidence mirrors are being developed and applied. The engineering of these elements is determined by accurate knowledge of optical constants of the materials involved and by the manufacturing accuracy. The major projects are reviewed. Finally, details and first results of the Hamburg focusing mirror scanning microscope are presented. With this instrument, imaging and microprobe analysis with less than 1μ resolution is possible in the energy range 20 - 1300 eV. Long term improvement could yield a resolution of 0.1 μm.

to be published in: Proceedings of the 15th Internat. Conf. on X-Ray and Inner Shell Processes, Knoxville, Tenn., July 9-13, 1990
AIP Conference Proceedings Series

INTRODUCTION

Nowadays there exists a host of different kinds of microscopies, each of them having its own merits. While the general goal of all microscopies is to achieve high resolution, they also display objects with different types of contrast. The idea to generate images with the use of x-rays came up soon after their discovery; it was, however, hampered by the fact that no lenses comparable to those in ordinary light optics exist. In spite of this many efforts have been made to overcome this problem[1] during the years. Practically all attempts are restricted to the soft x-ray regime, namely photon energies below about 1000 eV. Imaging can be achieved by Fresnel zone plates and by different types of mirrors. Further, scanning can sometimes be achieved with much simpler optics, in the simplest case by putting the sample behind a pin-hole. When a microfocus of soft x-rays is generated, not only transmission but also secondary processes like e.g. photoelectron emission, ion desorption, luminescence etc. may serve to obtain images. This type of microscopy has the advantage that often the observed contrast is readily interpreted in terms of fundamental physical processes. Finally, the electrooptical imaging of photoelectrons which are emitted from a wide range of the sample should also be mentioned.

The renewed interest in x-ray microscopy has several reasons. Maybe the most important is the advent of synchrotron radiation[2,3], especially from the third generation of storage rings[4-6] which will produce undulator radiation with unprecedented brightness. There are other developments in parallel which are of similar importance, improved x-ray optics namely zone plates, multilayer coated mirrors, and highly polished grazing incidence mirrors[7,8]. Further, new high resolution x-ray resists have been developed to be used as recording media for contact microscopy.

All these developments are well documented in a series of conference proceedings[9-11].

This fall scientists from all over the world will come together again for the International Symposium "X-Ray Microscopy III" in London September 3-7, 1990. At that time a full survey on recent progress will be available. In this paper the general ideas of x-ray imaging and a few selected examples will be presented. Any attempt like the one to which chapter I is devoted to list presumptive applications of x-ray microscopy must remain incomplete. Chapter II. addresses the performance and the fundamental limitations of x-ray microscopes derived from the properties of their optical elements. In chapter III. the most advanced existing microscopes are addressed. Finally, in chapter IV the Hamburg ellipsoidal mirror microscope, a project in which the author himself is involved, is described in some detail.

I. APPLICATIONS OF SOFT X-RAY MICROSCOPY

Before looking into the technical details of x-ray microscopy it appears to be appropriate to consider some possible applications. This would set minimum goals for the performances which need to be achieved. Practically all types of x-ray microscopes are still in a state which is far from a routine operation for the solution of real scientific or applied problems. Some of the potential applications discussed under these circumstances may turn out to become superseded by unforeseen difficulties or new competing techniques developed in the meantime. On the other hand, it is common experience that once a new tool becomes available, other unexpected possibilities will show up.

Quite generally, two directions can be foreseen for applying these microscopes: Any structured objects, where soft x-rays would provide a contrast revealing such structures or allowing that structural contrast to be quantified in a way not feasible by other means, could be investigated. The resolution, however, needs to be better than or at least in the order of the smallest structure of interest.

Another direction would involve all kinds of soft x-ray spectroscopies which are nowadays performed on macroscopic samples. The same spectroscopies could then be applied to microscopic samples or microscopic homogeneous spots on large samples.

Among structured samples one should primarily consider biological objects. Soft x-ray microscopy opens up the possibility to obtain images with good contrast of cells, nuclei, bacteria, etc. in their living state, i.e. in a thin film of aqueous solution, rather than dried and stained. First images of this type are now available with a resolution in the 50 nm range. This resolution is beyond that of the light microscope. X-ray microscopes built for this purpose do not require tunability over a large energy range but they could operate well at a fixed photon energy in the so-called "water window" (250-500 eV). Zone plate microscopes are appropriate at that energy because of their good resolution.

Once resolution becomes better and better for biological samples, radiation dosage increases in parallel since visibility of a certain structure depends on contrast and on the number of photons within the resolution interval. There is as yet an unresolved discussion going on about the amount of photon density biological objects of different types can tolerate before the image obtained is not any longer representative of a living structure. Since this could become a problem in the future, it should be noted that scanning transmission microscopy is advantageous in this respect compared to imaging microscopy. The reason is that in the latter case the useful number of photons is reduced by the typically low efficiency of the imaging element while in scanning microscopy all the transmitted photons are used.

With scanning microscopy in certain arrangements of the optical elements the topmost layers of solid samples can be investigated by means of secondary processes. Photoemitted electrons contain information from a depth between 1 and 10 monolayers depending on their

energy. A detailed energy analysis could be easily performed if sufficient intensity is available. In this case, information on the chemical elements residing in a surface layer as well as their chemical environment could be obtained by XPS. At the same time tuning of the photon energy could enhance signals and resolve ambiguities. Of course, one should not forget that there is a heavy competition with other imaging surface sensitive methods like e.g. imaging Auger-spectroscopy. Advantages and disadvantages of the different methods are, however, assessed in much the same way as with macroscopic probes.

Other processes such as photo-stimulated desorption of specific ions, fluorescence and scattered radiation could become even more important in the long run. Soft x-rays as a probe have the special advantage over electrons that insulating surfaces could be analysed without problems due to charge build up.

Once a small beam on the order of 1 μm contains enough photons to support a static spectroscopy like XPS etc., this would help in applying the methods to new materials which could be grown only in the form of tiny crystals or which do not have large homogenous surface areas. For example many of the new high T_c materials were produced initially as small crystals. Growing big crystals involves great efforts. Even those which are grown presently as large crystals have inhomogeneous cleavage surfaces. Dangerous materials or materials which have too high a vapour pressure for a good vacuum could be prepared as tiny thin layered spots on e.g. carbon foils in a separate system and, thereafter, be investigated by a microbeam. Damage to the instrument could be avoided this way while valuable data are obtained.

II. PERFORMANCE OF THE OPTICAL ELEMENTS

In this chapter we shall look into the fundamental limitations of optical elements used in imaging and in scanning soft x-ray

microscopy. Since no lenses are available for this spectral region, the only elements which come into consideration are Fresnel zone plates and mirrors. Mirrors could be covered with multi-layer coatings in order to form artificial Bragg-reflecting crystals. For shorter wavelengths, natural bent crystals could also be used. In order to be more specific, we consider a well defined example of scanning microscopy using undulator radiation from a storage ring in an arrangement given in fig. 1. The optical elements needed to

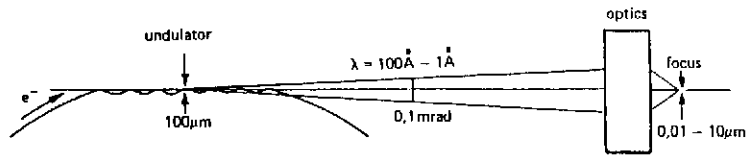

Fig. 1: Typical layout and parameters of a microfocus arrangement at an undulator in one of the next generation storage rings (from ref. 6)

generate a demagnified image of the source on the sample could be used in most cases (though not in all) in reverse to magnify a portion of the source on photographic film or resist.

With an undulator in one of the advanced newly planned storage rings radiation originates from a source with an effective source size of roughly 100 μm and a divergence of considerably less than 0.1 mrad. The goal is monochromatization to 0.1 eV unless the natural monochromaticity of undulator radiation of $\Delta\varepsilon/\varepsilon \cong 1{:}50$ is sufficient for certain types of experiments. In a next step radiation is to be focused down to a diffraction limited spot which should be as small as possible. There are fundamental limitations to the minimum spot size achievable and technical limitations to the manufacturing of the

optical elements. The technical limitations may be overcome step by step due to ingenuity or by investing enough effort and money.

We try now to obtain a rough estimate of the fundamental limitations. The final step of imaging onto the sample must be a large demagnification D of the source itself or of an intermediate image which is defined properly by a diaphragm. According to fig. 2 , D = d/d'= l/l'.

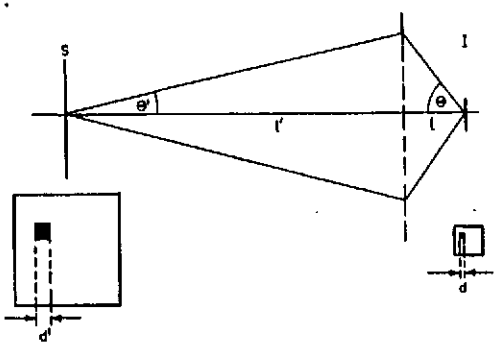

Fig. 2: Illustration to explain Liouville's theorem in a microfocus arrangement, S = source, I = image, d' and d are corresponding elements of S and I respectively (from ref. 6).

Then Liouville's theorem (in optics known as the Abbé condition)

$$d \sin \Theta = d' \sin \Theta' \qquad (1)$$

provides a relation for the angular widths Θ,Θ' in the case of perfect imaging. Further, a focus of diameter d requires a minimum angular width due to the coherence condition

$$2d \sin \Theta \cong \lambda. \qquad (2)$$

In agreement with the usual definition of the diffraction limit of the classical light microscope d means the FWHM of the central

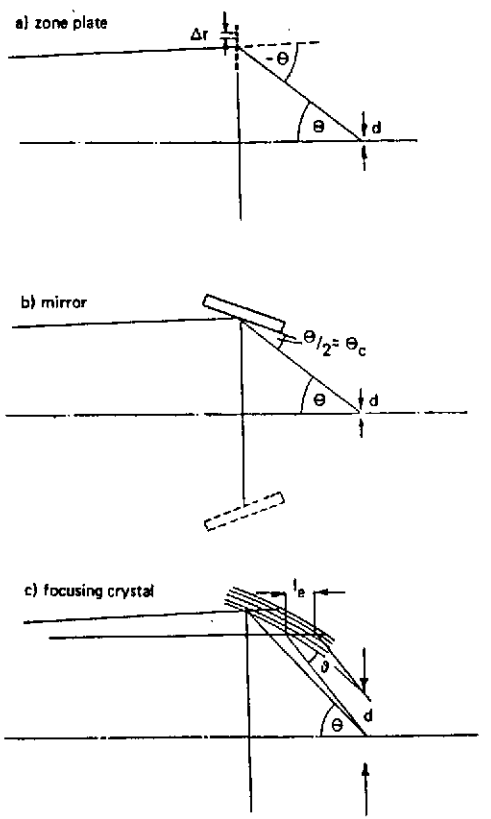

Fig. 3: Limitations to the smallest spot size d' attainable in a microfocus arrangement a) with a Fresnel zone plate with outermost zone separation Δr, b) with mirror optics (rotationally symmetric) with the critical angle of total reflection Θ_c, c) with a bent crystal with the extinction length l_e contributing to the spot size d, ϑ is the Bragg angle (from ref. 6).

diffraction peak which, for the purpose of this paper, is roughly approximated to lie within 20 % of the value given by eq. (2).

a) A Fresnel zone plate (see fig. 3) is a circular diffraction grating with the local grating constant Δr determined such that the beam is diffracted to the image point. The grating equation is

$$\Delta r(\sin\Theta - \sin\Theta') = m\lambda \qquad (3)$$

where m is the order of diffraction. When D is small, it follows that $\Theta' \cong 0$ and eq. (3) reads $\Delta r \sin\Theta = m\lambda$. With λ from eq. (2) and the local grating constant Δr_{min} of the of the outermost zone, we have

$$d \cong \Delta r_{min}/2m. \qquad (4)$$

Thus in first (m = 1) order the resolution is limited to the width of the outermost zone $\Delta r_{min}/2$. If one remembers that all zones must be concentric and spherical to within a fraction of $\Delta r_{min}/2m$, it is understandable that the present resolution of zone plates is limited to d ≅ 500 Å. Nevertheless, the production of zone plates with even lower dimensions of Δr_{min} appears to be a technical rather than a fundamental problem. In this context it should be remembered that the "dark" zones need to have a certain thickness t either in order to block the beam or in order to shift the phase of the radiation by $\lambda/2$. The latter is achieved in so called "phase zone plates" taking advantage of the very small deviation of the real part of the index of refraction of 1 in the 500 - 1000 eV range. The aspect ratio $2t/\Delta r_{min}$, however, becomes forbiddingly large with decreasing Δr_{min}.

b) Under the assumption that a single mirror constitutes the optical element in the final demagnification stage we arrive at an estimate for the grazing incidence region (photon energies above 100 eV). From a Drude model for the index of refraction we obtain $n = 1 - \omega_p^2/(2\omega^2) = 1 - \lambda^2/(2\lambda_p^2)$ with ω_p, λ_p being a plasma frequency and plasma "wavelength" respectively. Θ_c the grazing critical angle of

total reflection is defined by $\cos\Theta_c = n$. Θ_c is roughly the angle at which the reflectivity is 50 %. $n \cong 1 - \Theta_c^2/2$. For small Θ_c we have $\Theta_c \cong \lambda/\lambda_p$ and with $\Theta = 2\,\Theta_c$ (see fig. 3) in combination with eq. (2) we obtain

$$d \cong \lambda_p/4. \qquad (5)$$

This effective plasma wavelength gives only a rough representation of the optical constants in a certain spectral range. In principle λ_p should be inversely proportional to the square root of the number of "free" electrons per unit volume. In addition to the conduction electrons all those core electrons should be counted which can be excited at a given photon energy and which have exhausted their oscillator strength. Therefore, λ_p might decrease slowly with decreasing wavelength. In practice, however, reflectivities are well represented by a constant λ_p, which for gold coated mirrors gives $\lambda_p \cong 200$ Å over a wide energy range[13]. With this λ_p in eq. (5), we obtain the ultimate limit to the obtainable spot size of d ≅ 50 Å with a single mirror optics. With a double mirror optics, e.g. the Wolter type I arrangement[14-16] the limit could become half this value. Other limitations lie of course in the aberrations and in the manufacturing accuracy of mirror elements with complicated shapes.

c) Bent crystal optics and multilayer coated reflecting optics are limited to fixed photon energies, but with those elements grazing reflection angles can be made large. There is, however, the problem that the grazing angle of reflection ϑ and the wavelength λ are linked by Bragg's law.

$$2d_1 \sin\vartheta = m\lambda \quad , \qquad (6)$$

where d_1 is the lattice or multilayer spacing and m the order. Laterally graded lattice constants may be generated with multilayer coatings but not so easily with crystals. A near normal incidence optics like the Schwarzschild arrangement[17] is probably the optimum

for such elements. Due to the large scattering at normal incidence by surface roughness there is a serious technical problem in this arrangement (see eq. (9)) below.

Normal incidence will also minimize another limitation of such optics which is due to the finite depth in which radiation is reflected (see fig. 3). If 1_e is the extinction length the width of the focus due to this effect is

$$d = 1_e \frac{\sin \vartheta}{|\cos 2\vartheta|} \qquad (7)$$

Since 1_e can be in the order of 5000 Å this effect can seriously influence the size of the focal spot unless ϑ is less than a few degrees, or unless ϑ is equal to 90 ° within a few degrees (back reflection).

d) The simplest way to obtain a microfocus is by placing a pinhole in a parallel beam. The size of the light spot depends on the distance x between the pinhole of diameter d' and the sample. Then the size of the spot is given (see fig. 4) as:

$$d = d' + 2x\tan\Theta + x(\lambda/d') \qquad (8)$$

size divergence diffraction

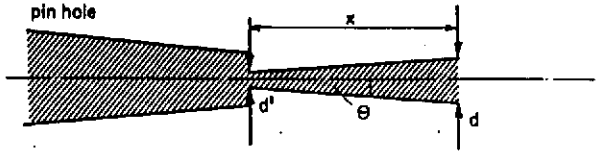

Fig. 4: Definition of the parameters of a pinhole scanning microprobe (from ref. 6).

We assume x = 5 mm, a distance barely large enough in order to be able to extract the photoelectrons from the sample surface. At λ = 20 Å and neglecting the divergency term, the optimum pinhole size is

then d' = 3 µm which yields a spot size of d = 6 µm. The divergency of the beam illuminating the pinhole would have to be $\Theta \leq 10^{-4}$ rad. This amounts, however, to a demagnification D = 1 of the undulator source onto the pinhole. The loss of intensity with an assumed source diameter of 100 µm corresponds to $(3\ \mu m/100\ \mu m)^2 \cong 10^{-3}$. All this is just a simple demonstration of where the limitations are for this simplest possible approach to spatially resolved photoemission. Nevertheless, in certain cases, e.g. photoemission on crystals which can only be grown in sizes up to 10 µm, this approach might make sense. Also with photon excited Auger analysis[18] which does not require monochromatization of the exciting radiation, such an approach might be reasonable.

Let us finally consider emittance/acceptance matching between the source in the storage ring and the spot on the sample (see fig. 1). If the source size of 100 µm as obtainable in third generation storage rings is demagnified by $D = 10^{-3}$ to a spot of 1000 Å the overall emission angle (electron beam divergence convoluted with the undulator angular distribution) which we assumed is $2\Theta = 10^{-4}$ rad transforms according to eq. (1) by a factor D^{-1} to $2\Theta = 10^{-1}$ rad. This amounts to an angle Θ = 3° or a grazing incidence reflection angle $\Theta/2$ = 1.5°. At λ = 10 Å, $\Theta_c = \lambda/\lambda_p$ = 3° for a Au coating is well above this angle. Even further demagnification is feasible without more loss of intensity than that due to the limited reflectivity of the optical elements.

One important factor in this context is the loss of specular reflectivity due to roughness. The actual reflectivity is calculated in the simplest theoretical approach from the reflectivity of a perfectly smooth surface R_o by

$$R = R_o \exp\{-[(4\pi\sigma\sin(\Theta/2))/\lambda]^2\} \qquad (9)$$

where σ is the mean square roughness with a Gaussian hight distribution. The scattered intensity is unfortunately not lost but generates

a diffuse background in the image of the sample which will reduce the contrast[19,20].

III. REALIZATIONS OF SX-MICROSCOPES

A fairly complete survey on all the projects underway in recent years worldwide is contained in book form as proceedings of two conferences on x-ray microscopy[10,12]. As mentioned in the introduction a third conference of this series will follow September 1990. Proceedings of some additional meetings have also been published[9,11]. Here only a few of the most advanced projects can be mentioned.

By far the most advanced project is that of the Göttingen group[9-12]. This group has developed both imaging (fig. 5) and

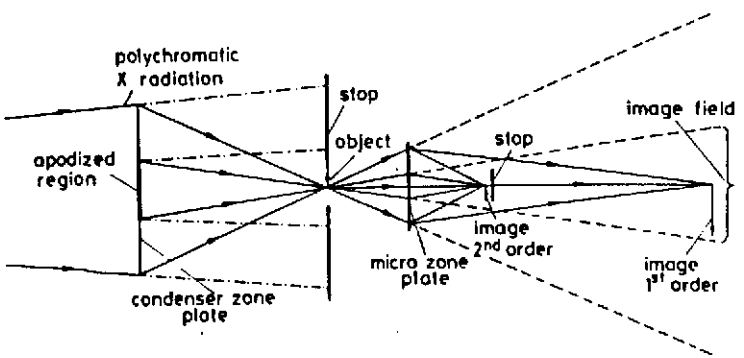

Fig. 5: Arrangement of the zone plate microscope
(from ref. 10 p. 196)

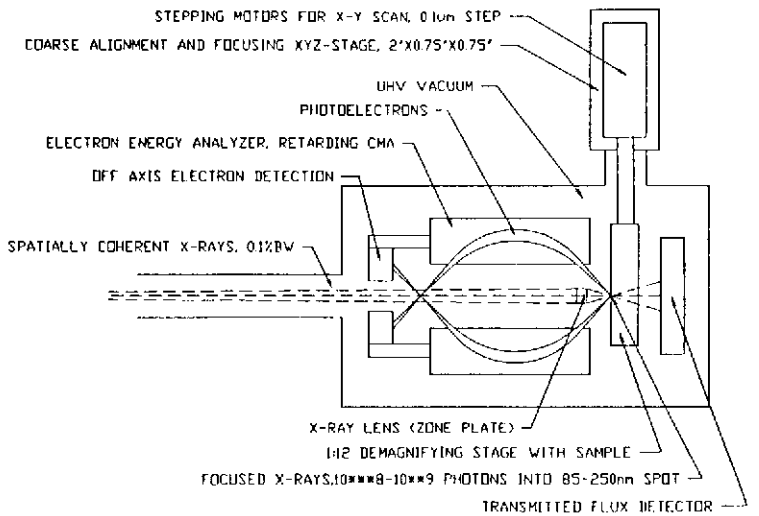

Fig. 6: The scanning XPS-microscope (from ref. 24)

scanning microscopy with holographically produced zone plates as optical elements. They apply this microscopy exclusively for the investigation of biological objects in the so-called water window between 250 and 500 eV photon energy. They have obtained a spatial resolution of 30 nm with an imaging microscope and of 50-60 nm with a scanning microscope, both installed at a bending magnet beam-line at the storage ring BESSY in Berlin. This group has obtained images of biological objects in a wet environment practically under living conditions. They work on several improvement programs as e.g. production of phase zone plates with increased efficiencies, phase contrast imaging[21] (in contrast to the common imaging of the

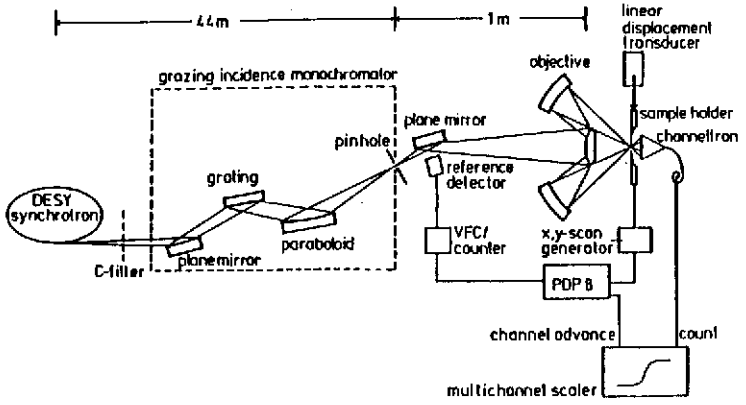

Fig. 7: Prototype of a scanning microscope installed at the original DESY synchrotron using a multi-layer coated Schwarzschild objective at $h\nu$ = 60 eV (from ref. 17)

absorption structure of the objects) and installation of a microscope illuminated with a plasma source. Recently they also succeeded in manufacturing a wet cell with controllable thickness of the water layer contained between two thin plastic foils.

Other well advanced zone plate microscopes, all of them in the scanning mode, are operated at Brookhaven[22] and at Daresbury[23]. The groups are located at Stony Brook and the Imperial College London respectively. Both use zone plates produced by e-beam writing taking advantage of modern methods developed for the production of micro-electronic circuits. Both groups have installed the microscopes at undulator beam lines. They have mainly investigated biological samples and other objects all in the transmission mode. In addition, Ade et al.[24] from Stony Brook have recently succeeded in operating a zone plate microscope in conjuction with a cylindrical mirror

analyzer (fig. 6) for scanning photoemission microscopy. They have obtained images of line structures of alternatingly Al, SiO_2 and Si on a silicon wafer. The resolution obtained is in the order of 0.3 µm.

In our laboratory Haelbich et al.[17] have developed a scanning microscope based on a Schwarzschild objective (fig. 7) coated with reflection enhancing multi-layers. At that time a resolution of 1 µm was obtained but intensity was low since neither a storage ring beam-line nor undulators were available.

This idea was recently revived in the MAXIMUM project at the ALADDIN storage ring in Wisconsin[25]. The MAXIMUM microscope has recently obtained 0.5 µm resolution at about 100 eV photon energy. Due to the exorbitant importance of surface roughness at normal incidence (see eq. (9)) this type of microscope will probably be restricted to maximum photon energies in the 100 eV region.

Photoemission microscopes with electron imaging are presently being developed by Tonner et al.[26] and King et al.[27]. Also several groups are developing such microscopes with classical light sources in the ultraviolett[28-30] where differences in work function at surfaces create a pronounced contrast.

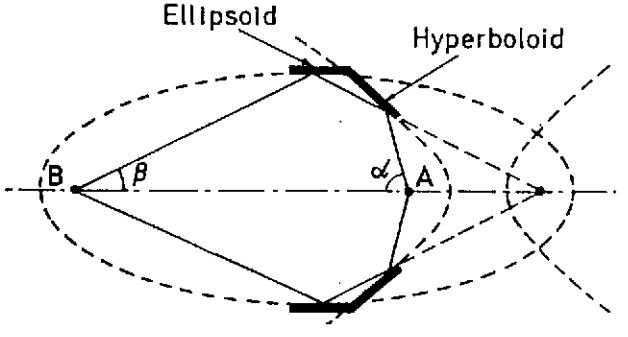

Fig. 8: Geometry of the Wolter I microscope (from ref. 16)

Aoki et al. 31 and Franks et al. 16 have obtained images using grazing incidence reflection from two consecutive surfaces in a Wolter[14,15] type arrangement (see fig. 8).

Some of these microscopes are intended for operation with sources other than synchrotron radiation. Images could be obtained with radiation from a laser produced plasma in one shot. In contrast to a zone plate microscope monochromaticity is not required and the full spectrum emitted by the source contributes to form an image.

IV. ELLIPSOIDAL MIRROR SCANNING MICROSCOPE

The simplest possible rotationally symmetric reflecting optical element is a rotational ellipsoid which collects radiation originating from one focal spot focusing it into the other one. Fig. 9 shows an arrangement which is presently set up at the HASYLAB laboratory by the University of Hamburg[32]. The elliptical ring mirror has a diameter of 5 mm; a length of 6 mm; distances 1' = 1000 mm;

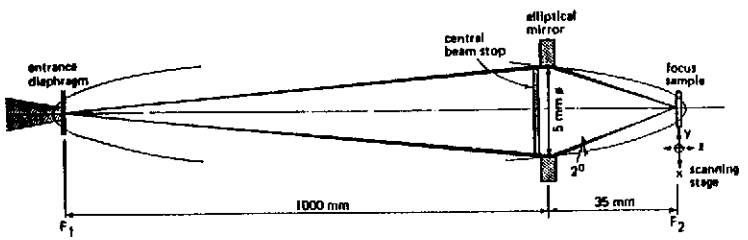

Fig. 9: Principle and parameters of the scanning photoelectron microscope under construction at HASYLAB. F_1, F_2 are the foci of the elliptical mirror (from ref. 6)

1 = 35 mm; a demagnification D = 1/30; and a grazing angle of reflection $\Theta/2 = 2°$. It reflects radiation up to $\varepsilon \cong 2000$ eV. The imaging properties are such that a point in the object plane at a

distance d' from the axis generates a whole circle with a radius d = Dd' in the image plane. This circle is concentric to the axis of the ellipsoid. Thus a concentric circle in the image plane is imaged on a concentric demagnified circle in the object plane and a concentric diaphragm of diameter d' has an image as a spot of diameter d = Dd'. For the purpose of forming a microfocus such a mirror fulfils all the necessary requirements. Also, calculations involving diffraction show that the diffraction pattern is close to that of an annular aperture of 5 mm diameter and 200 μm width. Therefore the general considerations mentioned above for the resolution limit due to diffraction apply. As a matter of fact due to the necessary apodization eq. (2) needs to be modified for a hollow cone yielding approximately

$$4d \sin\Theta = \lambda \tag{10}$$

As a consequence also eq. (5) is modified to

$$d \cong \lambda_p/8 \tag{11}$$

In the case of the ellipsoid microscope, with $\theta/2 = 0.035$ rad, we have $\theta/2 < \theta_c$ for photon energies below 2000 eV. Note that the resolution according to eq. (11) is only obtained at this upper limit in photon energy. The hollow cone diffraction pattern, although being narrower than that of a full cone, has the disadvantage that the central diffraction peak contains less than 10% of the total intensity depending on the length of the mirror. The rest is smeared out into the diffraction rings of higher order and will generate a background in the vicinity of each resolution element. With the phase I microscope which is now operating at HASYLAB, a 30 μm diameter diaphragm is demagnified to a d = 1 μm diameter image. Because of the imperfections of this first mirror (manufactured by the Zeiss company with the best presently available technology) it is not yet worthwhile to operate the instrument with a 10 μm diaphragm which would yield a focus of 0.3 μm. This has to be compared with the diffraction limit according to eq. (10) with $\theta = 0.14$ rad yielding at $\lambda = 20$ Å; d =

0.014 μm. Thus in this phase of the project there is no limitation to be expected due to diffraction. In a phase II which aims at a focus of 0.1 μm this mirror will reach the diffraction limit of 0.1 μm at λ = 170 Å corresponding to ε = 75 eV.

This microscope is installed behind the FLIPPER station[33] at the W1 undulator at HASYLAB. It can be operated with one single alignment in the whole range ε = 20-1300 eV, its angular acceptance is matched to that of the FLIPPER monochromator. The overall intensity loss is a factor of 10^{-3} (10 μm diaphragm, 300x250 μm^2 spot size), and a geometrical acceptance factor of $1.25 \cdot 10^{-2}$ at the mirror. The specular reflectivity of the mirror will depend on its roughness. Some initial tests on prototype mirrors together with tests on the actual mirrors are encouraging. Assuming an optimistic value of R = 0.8, we obtain a general loss factor of 10^{-5} by which the intensity at the exit slit of the monochromator needs to be multiplied. At the maximum intensity of the FLIPPER (100 eV, $2 \cdot 10^{13}$ Photons) we would obtain $2 \cdot 10^{8}$, and at the oxygen K-edge (534 eV) approximately 10^{7} photons are available.

Possible gains in intensity at third generation storage rings of lower emittances with monochromators equipped with better optical elements are roughly estimated: a factor of 10 at the entrance aperture, a factor of 5 with a smaller horizontal divergence and a factor of 20 using longer undulators with more periods. Thus three orders in magnitude in the gain appear to be a reasonable estimate due to improvements of the storage rings. Using somewhat longer mirrors or mirrors with higher angles θ/2, one could also gain some intensity but to a lesser extent. It should, however, be mentioned that using such a small angle as θ/2 = 2° for longer wavelengths enhances specular reflection and reduces roughness scattering according to eq. (9).

The ellipsoidal mirror microscope is operated at HASYLAB, Hamburg, since 1989. Several different mirrors have been tested and

characterized up to now. At this moment, an ellipsoidal mirror is available which produces a focal spot of a little less than 1 μm FWHM. The intensity distribution is not Gaussian but has wings which contain a non-negligible fraction of the intensity. The overall intensity behaves as estimated above. Under specific conditions intensities between $5 \cdot 10^{5}$ and $7 \cdot 10^{7}$ photons/sec. were obtained between 30 and 600 eV photon energy as measured by a calibrated Schottky barrier detector.

Images of test objects as shown in fig. 10 and 11 are obtained for different photon energies between 50 and 1100 eV both in transmission and photoelectric yield. The signals are either measured with channeltrons or with solid state detectors.

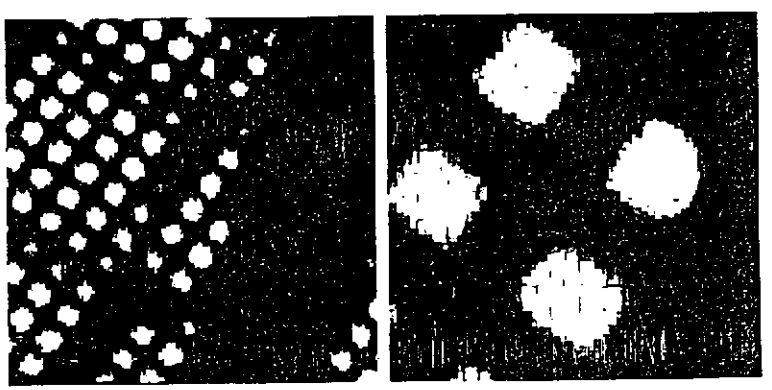

Fig. 10: Transmission of a fine Cu grid, partly obstructed by a coarser supporting grid, left side, 133 μm x 142 μm, right side 27 μm x 21 μm, hν = 260 eV.

Recently we were also able to obtain first XPS spectra with a spherical electron analyser equipped with a special electron lens. A spot of 3 μm diameter was kept fixed on SiO_2 and Au samples.

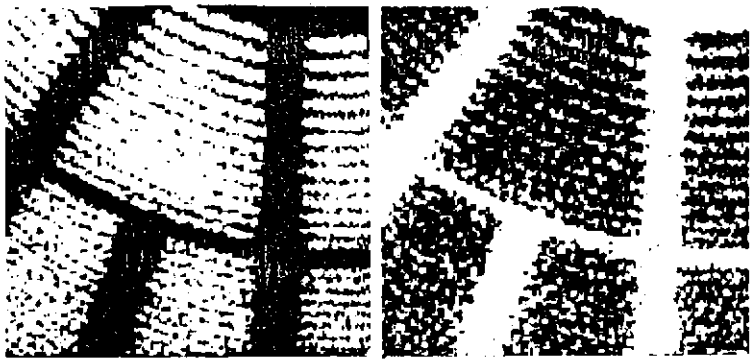

Fig. 11: Section of a Fresnel zone plate, 135 μm x 142 μm, left side transmission, right side total electron yield, hν = 260 eV.

The mechanics of the microscope and the scanning stage are designed and manufactured with great care so that images down to 0.1 μm resolution could be obtained once a sufficiently accurate ellipsoidal mirror is available. The details of the microscope are described elsewhere[31].

I want to thank Dipl.Phys. Joachim Voβ and Dr. Cullie Sparks[32] for a critical reading of the manuscript and E. Lücke and S. Weigert for their help in preparing the manuscript.

REFERENCES

1 V.E. Cosslett and W.C. Nixon, X-ray Microscopy (Cambridge University Press 1960)

2 E.E. Koch, Ed., Handbook on Synchrotron Radiation (North Holland, Amsterdam, New York, Oxford, 1983) Vol. 1a,1b,2

3 C. Kunz, Ed., Synchrotron Radiation - Techniques and Applications (Springer, Berlin, Heidelberg, New York, 1979) Topics in Current Physics, Vol. 10

4 M. Ando, T. Miyahara Eds., Proceedings of the 3rd Int. Conf. on Synchrotron Radiation Instrumentation, SRI 88 (Tsukuba, 29. Aug.-2. Sept. 1988), Rev. Sci Instrum 60, 1373 1989

5 R.C.C. Perera and A.C. Thompson Eds., Proceedings of the Sixth National Conference on Synchrotron Radiation Instrumentation (Berkely 7.-10. Aug. 1981) Nucl. Instr. Meth. Phys. Res. Vol. A291, 1990

6 C. Kunz, Proc. Int. School of Physics "Enrico Fermi" (Varenna July 12-22, 1988) in press

7 E. Spiller, Ed., High Resolution Soft X-Ray Optics (Conf. Brookhaven 18-20 Nov. 1981) Proc. SPIE 316 (1981)

8 E.E. Koch, G. Schmahl, Eds., Soft X-Rays Optics and Technology (Conf. Berlin 8-11 Dec. 1986) Proc. SPIE 733 (1986)

9 D.F. Parsons, Ed., Ultrasoft X-Ray Microscopy, Its Application to Biological and Physical Sciences (New York 13-15 June 1979) Annals of the New York Academy of Sciences, Vol. 342 (1980)

10 G. Schmahl, D. Rudolph, Eds., Proceedings of the International Symposium, X-Ray Microscopy (Göttingen, 14-16 Sept. 1983) Springer Series in Optical Sciences 43 (Springer, Berlin, Heidelberg 1984)

11 Ping-chin Cheng, Gwo-jen Jan, Eds., X-Ray Microscopy - Instrumentation and Biological Applications (Proceedings Symposium, Taipei Aug. 1986) (Springer, Berlin, Heidelberg 1987)

12 D. Sayre, M. Howells, J. Kirz, H. Rarback, Eds., Proceedings of the International Symposium, X-Ray Microscopy II (Brookhaven 31 Aug. - 4 Sept. 1987) Springer Series in Optical Sciences 56 Springer Berlin, Heidelberg 1988)

13 B.L. Henke, P. Lee, T.J. Tanaka, R.L. Shionabukuro, B.K. Fujikawa, Atomic Data and Nuclear Data Tables 27, 123 (1982)

14 M. Wolter, Ann. Phys. 10, 94 (1952)

15 M. Wolter, Ann. Phys. 10, 286 (1952)

16 A. Franks, B. Gale, in Ref. 10, p. 129

17 R.P. Haelbich, W. Staehr, C. Kunz, in Ref. 9, p. 148

18 E. Umbach, Z. Hussain, Phys. Rev. Lett. 52, 457 (1984) and private communication

19 H. Hogrefe, C. Kunz, Appl. Optics 26, 2851 (1987)

20 H.G. Birken, C. Kunz, R. Wolf, Physica Scripta 41, 385 (1989)

21 G. Schmahl, D. Rudolph, P. Guthmann, in Ref. 10, p. 228

22 J. Kirz, M. Ade, E. Anderson, D. Attwood, C. Buckley, S. Hellmann, M. Howells, C. Jacobsen, D. Kern, S. Lindaas, I. McNulty, M. Oversluizen, H. Rarback, M. Rivers, S. Rothman, D. Sayre, D. Shu, Physica Scripta T31, 12 (1990)

23 G.R. Morrison, M.T. Browne, C.J. Buckley, R.E. Burge, R.C. Cave, P. Charalambons, P.J. Duke, A.R. Hare, C.P.B. Hills, J.M. Kenney, A.G. Michette, K. Ogawa, A.M. Rogoyski, T. Taguchi in ref. 12, p. 201

24 H. Ade, J. Kirz, S.L. Hulbert, E.D. Johnson, E. Anderson, D. Kern, Appl. Phys. Lett. 56, 1841 (1990)

25 G. Margaritondo, private communication

26 G.R. Marp, Z.-L. Man, B.P. Tonner; Physica Scripta T31, 23 (1990)

27 P. Pianetta, I. Lindau, P.L. King, M. Keenlyside, G. Knapp, R. Browning, Rev. Sci. Instrum. 60, 1686 (1989)

28 W. Telieps, E. Bauer, Ultramicroscopy 17, 57 (1985)

29 F. Polack, S. Lowenthal, D. Phalippou, P. Fournet, in Ref. 10, p. 220

30 H. Bethge, T. Krajewski, O. Lichtenberger, Ultramicroscopy 17, 21 (1985)

31 S. Aoki, in ref. 12, p. 102

32 J. Voß, H. Dadras, C. Kunz, A. Moewes, R. Roy, H. Wongel, H. Sievers, I. Storjohann, to be published

33 F. Senf, K. Berens v. Rautenfeldt, S. Cramm, J. Lamp, J. Schmidt-May, J. Voß, C. Kunz, V. Saile, Nucl. Instrum. Meth. A246, 314 (1986)